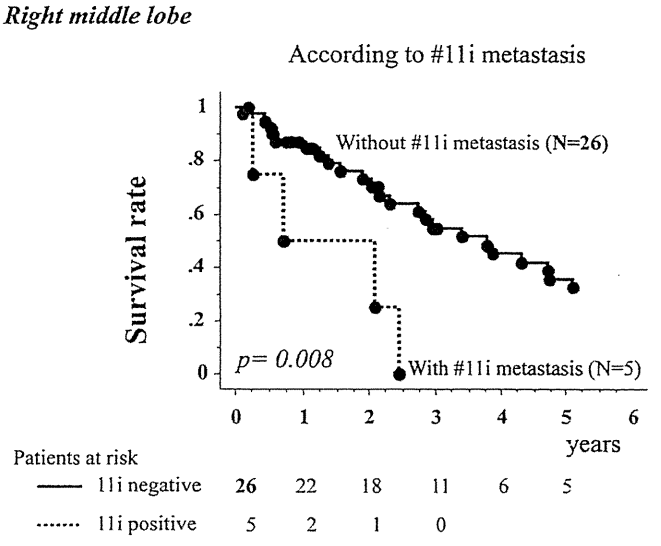

FIGURE 7. Postoperative survival according to #11i nodal involvement.

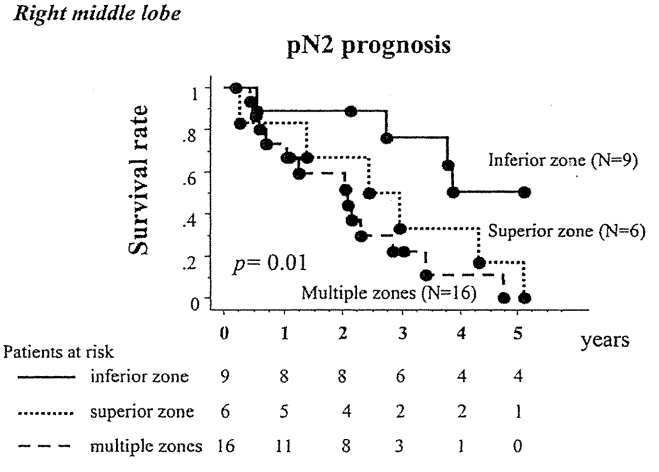

FIGURE 8. Postoperative survival: comparison of superior mediastinal nodal involvement with multiple-zone metastases.

node metastases were revealed to be a stronger prognostic factor than multiple metastatic zones (Figure 8).

DISCUSSION

There have been many reports on the prognostic impact of metastasis to specific mediastinal zones, especially lung cancer in the upper or lower lobes. For patients with lung cancer with tumor originating in the upper lobe or division, the frequency of subcarinal lymph node metastases has been reported to range from 3 to 5%, with the 5-year survival rates ranging from 9 to 18%.[8–10] The frequency of superior mediastinal lymph node metastases has been reported to range from 4 to 5%, with 5-year survival rates ranging from 0 to 19%.[10,11] This low-frequency mediastinal lymph node involvement was highly associated with multilevel N2, and therefore, the outcomes were poor.[10,12,13] In this study, the frequency of metastases was similar for the subcarinal and superior mediastinal zones, and the incidences in N2 patients were 80.6% and 71.0%, respectively. Thus, both superior and inferior mediastinal zones were found to be major metastatic sites, and these results are compatible with previous reports.[14]

We have revealed that metastases to the superior mediastinal lymph nodes are an important independent prognostic factor in patients with N2 middle lobe cancer. This is similar to what is seen in lower lobe cancer. Nevertheless, the incidence of skip metastasis to the superior mediastinum is very different between cancer in the middle lobe and in the lower lobe. The incidence in this study was 20% for N2 and has been reported to range from 3 to 4.5% in N2 right lower lobe cancer.[10–12] Furthermore, there was a significant difference in the 5-year survival rates for superior mediastinal involvement and inferior mediastinal involvement (6.5% and 50.8%, respectively), even for single-zone N2. When superior mediastinal lymph nodes were involved, the prognosis was almost the same as for multilevel N2 patients with middle lobe cancer.

The most frequent metastatic hilar lymph node was #12m, and most #11s and #11i metastases were found in N2 patients. In other words, metastases found in #11s or #11i indicate N2 disease (#11s: 8/9 and #11i: 5/5). Surprisingly, interlobar (lower lobe: #11i) lymph node involvement was an important adverse prognostic factor, even in N2 patients. This may be explained by the fact that there was an association between #11i metastases and superior mediastinal nodal involvement. Metastasis in #11i may be understood to be a result of mediastinal nodal involvement. That is, #11i metastasis is retrograde because of disturbed antegrade lymph drainage to the superior mediastinum from mediastinal metastases. Unfortunately, we could not find any previous reports regarding this correlation between #11i and superior mediastinal node involvement. Further investigation is needed to prove the hypothesis that #11i metastases result from superior mediastinal lymph node metastases.

In conclusion, superior mediastinal lymph node metastases and #11i metastases were significant adverse prognostic factors in patients with middle lobe lung cancer, and they were associated with each other. Furthermore, in patients with middle lobe lung cancer, #11i metastases may result from mediastinal metastases, and the impact on prognosis must be different from that of patients with cancer in other lobes.

Limitations of this study include its retrospective nature, including cases from the 1980s, a small sample number, and that routine adjuvant chemotherapy for N2 patients was started in 2006. Therefore, in this study, it was difficult to evaluate the effects on prognosis with respect to adjuvant chemotherapy.

REFERENCES

1. Vincent RG, Takita H, Lane WW, et al. Surgical therapy of lung cancer. *J Thorac Cardiovasc Surg* 1976;71:581–591.
2. Freise G, Gabler A, Liebig S. Bronchial carcinoma and long-term survival. Retrospective study of 433 patients who underwent resection. *Thorax* 1978;33:228–234.

3. Gifford JH, Waddington JKB. Review of 464 cases of carcinoma of lung treated by resection. *Br Med* 1957;30:723–730.
4. Ochsner A, Ray CJ, Acreea PW. Cancer of lung; review of experiences with 1457 cases of bronchogenic carcinoma. *Am Rev Tuberc* 1954;70:763–783.
5. Riquet M, Dupont P, Hidden G, et al. Lymphatic drainage of the middle lobe of the adult lung. *Surg Radio Anat* 1990;12:231–233.
6. Hata E, Hayakawa K, Miyamoto H, et al. Rationale for extended lymphadenectomy for lung cancer. *Thorac Surg* 1990;5:19–25.
7. Rusch VW, Asamura H, Watanabe H, et al. Members of IASLC Staging Committee. The IASLC lung cancer staging project: a proposal for a new international lymph node map in the forthcoming seventh edition of the TNM classification for lung cancer. *J Thorac Oncol* 2009;4:1043–1045.
8. Asamura H, Nakayama H, Kondo H, et al. Lobe-specific extent of systematic lymph node dissection for non-small cell lung carcinomas according to a retrospective study of metastasis and prognosis. *J Thorac Cardiovasc Surg* 1999;117:1102–1111.
9. Uehara H, Okumura S, Satoh Y, et al. Validity of omission of subcarinal lymph node dissection in patients with cancer of the right upper lobe or left upper division of the lung. *Jpn J Lung Cancer* 2008;48:266–272.
10. Okada M, Sakamoto T, Yuki T, et al. Border between N1 and N2 stations in lung carcinoma: lessons from lymph node metastatic patterns of lower lobe tumors. *J Thorac Cardiovasc Surg* 2008;129: 825–830.
11. Uehara H, Sakao Y, Mun M, et al. Prognostic value and significance of subcarinal and superior mediastinal lymph node metastasis in lower lobe tumours. *Eur J Cardiothorac Surg* 2010;38:498–502.
12. Ichinose Y, Kato H, Koike T, et al. Japanese Clinical Oncology Group. Completely resected stage IIIA non-small cell lung cancer: the significance of primary tumor location and N2 station. *J Thorac Cardiovasc Surg* 2001;122:803–808.
13. Sakao Y, Miyamoto H, Yamazaki A, et al. The prognostic significance of metastasis to the highest mediastinal lymph node in non-small cell lung cancer. *Ann Thorac Surg* 2006;81:292–297.
14. Naruke T, Tsuchiya R, Kondo H, et al. Lymph node sampling in lung cancer: how should it be done? *Eur J Cardiothorac Surg* 1999;16:S17–S24.

Cancer Science
The official journal of the Japanese Cancer Association JCA

Analysis of HLA-A24-restricted peptides of carcinoembryonic antigen using a novel structure-based peptide-HLA docking algorithm

Yoji Nakamura,[1,2] Sachiko Tai,[1] Chie Oshita,[1] Akira Iizuka,[1] Tadashi Ashizawa,[1] Shuji Saito,[3] Shigeki Yamaguchi,[3] Haruhiko Kondo,[4] Ken Yamaguchi[1] and Yasuto Akiyama[1,5]

[1]Immunotherapy Division, Shizuoka Cancer Center Research Institute, Shimonagakubo, Nagaizumi-cho, Sunto-gun, Shizuoka; [2]National Research Institute of Fisheries Science, Fisheries Research Agency, Fukuura, Kanazawa, Yokohama, Kanagawa; [3]Division of Colon and Rectal Surgery, [4]Division of Thoracic Surgery, Shizuoka Cancer Center Hospital, Shimonagakubo, Nagaizumi-cho, Sunto-gun, Shizuoka, Japan

(Received November 8, 2010/Revised December 27, 2010/Accepted December 27, 2010/Accepted manuscript online January 13, 2011/Article first published online February 20, 2011)

Carcinoembryonic antigen (CEA) is a very common tumor marker because many types of solid cancer usually produce a variety of CEA and a highly sensitive measuring kit has been developed. However, immunological responses associated with CEA have not been fully characterized, and specifically a weak immunogenicity of CEA protein as a tumor antigen is reported in human leukocyte antigen (HLA)-A24-restricted CEA peptide-based cancer immunotherapy. These observations demonstrated that immunogenic and potent HLA-A24-restricted CTL epitope peptides derived from CEA protein are seemingly difficult to predict using a conventional bioinformatics approach based on primary amino acid sequence. In the present study, we developed an *in silico* docking simulation assay system of binding affinity between HLA-A24 protein and A24-restricted peptides using two software packages, AutoDock and MODELLER, and a crystal structure of HLA-A24 protein obtained from the Protein Data Bank. We compared the current assay system with HLA–peptide binding predictions of the bioinformatics and molecular analysis section (BIMAS) in terms of the prediction capability using MHC stabilization and peptide-stimulated CTL induction assays for CEA and other HLA-A24 peptides. The MHC stabilization score was inversely correlated with the affinity calculated in the docking simulation alone ($r = -0.589$, $P = 0.015$), not with BIMAS score or the IFN-γ production index. On the other hand, BIMAS was not significantly correlated with any other parameters. These results suggested that our *in silico* assay system has potential advantages in efficiency of epitope prediction over BIMAS and ease of use for bioinformaticians. (*Cancer Sci* 2011; 102: 690–696)

The carcinoembryonic antigen (CEA) is a very common tumor marker because many types of solid cancer usually produce a variety of CEA and a highly sensitive measuring kit has been developed.[1–3] However, immunological responses associated CEA have not been fully characterized except the observation that human leukocyte antigen (HLA)-A2 CEA epitope has been identified and contributed moderately to cancer vaccinations,[4,5] because there are several issues to be investigated. Specifically: (i) there are few efficient CEA epitopes with HLA-A24 restriction inducing cytotoxic T-lymphocytes (CTL) reaction in cancer patients; (ii) there have been few attempts to induce CEA-specific CTL using cancer patient-derived peripheral blood mononuclear cells (PBMC); and (iii) there have been few successful clinical trials using HLA-A24 restricted, which is well known as CEA peptide-based cancer vaccines.

Additionally, a weak immunogenicity or immunotolerance of CEA protein as a tumor antigen has been reported in cancer patients with advanced clinical stages.[6–8] Basically, CEA is originally expressed in the thymus and belongs to the CD66 family, which comprises highly homologous molecules expressed on hematopoietic cells, raising concerns about tolerance interfering with the development of anti-CEA immunity. Pickford *et al.*[6] reported that some effector T cells in PBMC can proliferate and some regulatory T cells can produce interleukin (IL)-10 with the stimulation by CEA protein using PBMC from 50 healthy volunteers. On the other hand, Crosti *et al.*[7] showed four CEA helper epitopes stimulating the proliferation of $CD4^+$ T-lymphocytes from end-stage lung cancer patients. These results supported that CEA tolerance could be overcome by peptide vaccine recognized specifically by effector T cells.

Nukaya *et al.*[9] reported CEA_{652}-A24-restricted peptide (TYACFVSNL) using healthy donor PBMC-based CTL induction assay for the first time and demonstrated that peptide-stimulated CTL efficiently killed CEA-positive cancer cell lines. The clinical trial by Matsuda *et al.*[10] and other researchers[11–13] using CEA_{652} peptide-treated dendritic cell (DC) vaccine showed that no significant clinical responses were seen, but some of the patients given vaccines developed *in vitro* CTL response against CEA peptide after vaccination. Considering that any HLA-A24 immunogenic CEA peptides besides CEA_{652} have not yet been found, it seems difficult to identify and predict immunogenic and potent HLA-A24-restricted CTL epitope peptides derived from CEA using conventional bioinformatics approach like HLA binding predictions of the bioinformatics and molecular analysis section (BIMAS) (http://www-bimas.cit.nih.gov/molbio/hla_bind/).

In the present study, we developed an *in silico* assay system to assess the affinity between HLA-A24 protein and A24-restricted peptide binder by combining two free software packages, protein 3D structure prediction software, MODELLER,[14] and protein-ligand docking simulation software, AutoDock.[15] In this method, we used a complex structure of HLA-A24 protein and its epitope peptide deposited in the Protein Data Bank (PDB)[16] as a template of 3D structure backbone. We then compared the current simulation assay with BIMAS in terms of the prediction capability and investigated the correlation of simulation results with other biological assays regarding HLA-A24 epitope binding.

Materials and Methods

Reagents and cell lines. Recombinant human (rh) granulocyte macrophage colony-stimulating factor (GM-CSF), rhIL-2, rhIL-4, rhIL-7 and tumor necrosis factor (TNF)-α were purchased (Pepro Tech Inc., Rocky Hill, NJ, USA). The GM-CSF, IL-4 and TNF-α were used at 10 ng/mL for dendritic

[5]To whom correspondence should be addressed. E-mail: y.akiyama@scchr.jp

doi: 10.1111/j.1349-7006.2011.01866.x

cell (DC) cultures. The TISI cell line was purchased (American Type Culture Collection, Manassas, VA, USA). Mouse anti-human HLA-A24 monoclonal antibody (MoAb) and FITC-labeled anti-mouse IgG were purchased (One Lamda, Canoga Park, CA, USA and Pharmingen, San Diego, CA, USA).

Synthetic peptides. CEA peptide sequences with HLA-A24 binding motif were searched at the website of BIMAS as HLA–peptide binding predictions. The top 10 peptides (Table 1) were selected and synthesized using the method reported by Knorr *et al.*[17] The sequences of other synthetic peptides used in the present study are CMVpp65$_{341–349}$ (QYDPVAALF), HIV-gp120$_{584–592}$ (RYLRDQQLL), MAGE-1$_{135–143}$ (NYKHCFPEI), MAGE-2$_{156–164}$ (EYLQLVFGI), MAGE-3$_{195–203}$ (IMPKAGLLI), gp100$_{152–160}$ (VWKTWGQYW), tyrosinase$_{206–214}$ (AFLPWHRLF), EBNA3A$_{246–254}$ (RYSIFFDYM), WT1-1M$_{235–243}$ (CYTWNQMNL), WT1-2$_{235–243}$ (CMTWNQMNL), HER2-1$_{63–71}$ (TYLPTNASL) and HER2-2$_{780–788}$ (PYVSR LLGI).

MHC stabilization assay. The protocol of MHC stabilization assay was described previously.[18] Briefly, 2×10^5 of T2-A24 cells suspended in 200 μL Iscove's modified Dulbecco's medium (IMDM; Gibco, Paisley, UK) containing 0.1% FBS were incubated with each peptide at 10 μM at 26°C for 16 h, and at 37°C for 3 h. The cells were stained with mouse anti-HLA-A24 MoAb and FITC-labeled anti-mouse IgG, and analyzed on a flow cytometer. Mean fluorescence intensity (MFI) increase was calculated as follows: MFI increase = (MFI with the given peptide − MFI without peptide)/(MFI without peptide).

CTL induction cultures. Thirty two cases of HLA-*A*2402*$^+$ cancer patients who showed more than 10 ng/mL of plasma CEA level, consisting of four lung and 28 colon cancer patients, were enrolled in the present study. Based on the collected cell number, finally PBMC from 29 cases of 32 were used for *in vitro* CTL inductions. The clinical research using PBMC from patients was approved by the Institutional Review Board of Shizuoka Cancer Center, Shizuoka, Japan. All patients gave written informed consent.

Briefly, PBMC were incubated in 6-well culture plates (Corning Inc., Corning, NY, USA) at 4×10^6 cells/mL in RPMI1640 medium supplemented with L-glutamine (2 mM), penicillin (100 U/mL), streptomycin (100 U/mL) and 5% (v/v) AB human serum (Lonza, Basel, Switzerland), referred to as DC medium, for 90 min. After incubation, the non-adherent cells were removed and the adherent monocyte-enriched population was cultured in the presence of 10 ng/mL of GM-CSF and 10 ng/mL of IL-4. On day 5 of culture, TNF-α was added at the dose of 10 ng/mL. After 7 days culture, most DC were positive for maturation markers like CD83, CD80, CD86, CD11c and HLA-DR in FACS analysis (data not shown). Harvested DC were suspended with Dulbecco's PBS with calcium and magnesium (referred to as PBS[+]) containing 1% human serum albumin (Kaketsuken, Kumamoto, Japan) and incubated with various HLA-A24 peptides (each final 25 μg/mL) for 2 h at 37°C. The DC were irradiated (30 Gy) and incubated with non-adherent autologous PBMC at a ratio of 1:50~100 in the presence of 10 ng/mL of IL-7. After 7 days of culture, the PBMC were restimulated with irradiated peptide-pulsed DC again and incubated for 1 week. Human IL-2 was added to PBMC cultures every 2–3 days at a final dose of 2.5 ng/mL. After two rounds of *in vitro* DC stimulation, PBMC were used for negative selection with anti-CD4 and anti-CD56 MoAb (BD Biosciences, Franklin Lakes, NJ, USA) on AutoMACS (Miltenyi, Gradbach, Germany). Finally, 29 cases of enriched CD8$^+$ T cells were used for IFN-γ production assay.

Table 1. CEA peptide sequences with HLA-A24 binding motif

Peptide name	Amino acid sequence	Position	Amino acid length	BIMAS score
CEA A24-1	TYYRPGVNL	425–433	9	200
CEA A24-2	TYACFVSNL	652–660	9	200
CEA A24-3	VYAEPPKPF	318–326	9	120
CEA A24-4	IYPNASLLI	101–109	9	75
CEA A24-5	LYGPDAPTI	234–242	9	60
CEA A24-6	LYGPDTPII	590–598	9	60
CEA A24-7	QYSWRINGI	624–632	9	60
CEA A24-8	LYGPDDPTI	412–420	9	60
CEA A24-9	TFQQSTQEL	276–284	9	39.6
CEA-A24-10	KTITVSAEL	492–500	9	18.5
CMVpp65 A24	QYDPVAALF	341–349	9	168

IFN-γ production assay. The TISI cells were incubated with HLA-A24 peptide overnight at 20 μg/mL suspended in PBS(+) containing 1% human serum albumin and used as target cells. Cultured PBMC (1×10^5) and HLA-A24 peptide-pulsed TISI cells (1×10^5) were co-incubated in a round-bottomed 96-well microculture plate for 24 h. Finally, supernatants were collected and IFN-γ levels were measured using an ELISA kit specific for human IFN-γ (Biosource, Camallilo, CA, USA). The IFN-γ production index was calculated as follows: IFN-γ production index = (IFN-γ level with the given peptide)/(IFN-γ level without peptide).

Establishment of *in silico* docking simulation assay for epitope peptide binding to HLA-A24 protein. First, we obtained a crystallized complex structure of HLA-A24 protein and its epitope peptide from PDB. The PDB code is 2BCK, which is currently only available as a 3D structure of HLA-A24 protein. The original epitope is a 9-mer peptide (VYGFVRACL) from human telomerase reverse transcriptase (hTERT). To build an initial 3D structure of any given A24-restricted epitope candidate peptide, we used the homology-modeling software, MODELLER (version 9v5) (University of California, San Francisco, CA, USA) with structure of hTERT epitope as a backbone template. Then, we predicted the affinities between HLA-A24 protein and synthesized peptides (see above) by receptor-ligand docking simulation software based on Lamarckian genetic algorithm, AutoDock (version 4.0) (The Scripps Research Institute, La Jolla, CA, USA). In AutoDock, an affinity between receptor and ligand molecules is calculated as the Gibbs free energy of binding (ΔG). Since the epitope-binding pocket on HLA protein and mode of binding have already been investigated,[19] the conformational search space in the AutoDock simulation can be limited to the vicinity of the HLA pocket by reference to the 2BCK data. Thus, the grid center coordinate defined in the search space was determined according to that of the original hTERT peptide and the size of the grid box was set to the default plus three points on each side of cuboid. For each of epitope candidate peptides, after Kollman charges are added, the docking simulations to HLA-A24 protein were run 50 times in each of which 1×10^6 energy evaluations were performed based on a genetic algorithm. Finally, we obtained the mean of top three affinities (the three lowest ΔGs) among the 50 runs as an affinity value of peptide binding.

Statistical analysis. The correlation coefficient, r, was calculated and statistical difference was analyzed using the Pearson's correlation test. Values of $P < 0.05$ were considered statistically significant.

Results

MHC stabilization assay of potential HLA-A24-binding peptides within CEA protein. The MHC stabilization assay was performed to test CEA and other protein-derived peptide candidates with HLA-A24-binding motifs for HLA-A2402 binding efficiency using T2-A24 cells. Stabilization efficiency was evaluated as high in one (MFI increase ≥ 3), medium in three

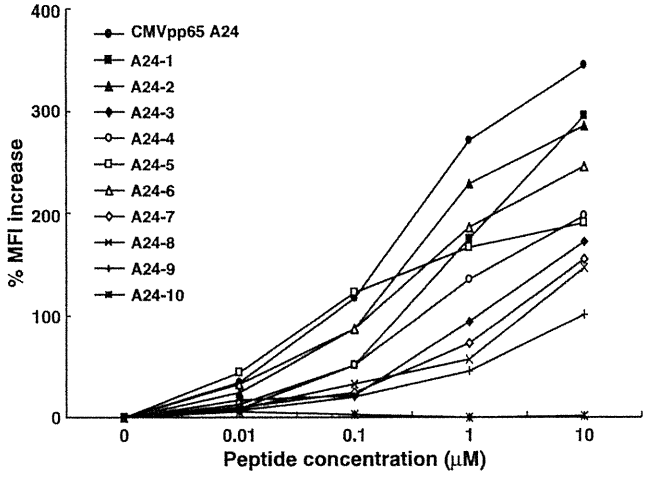

Fig. 1. A MHC stabilization assay of potential HLA-A24-binding peptides within CEA protein. The MHC stabilization assay was performed to check the binding affinity of CEA-derived peptides candidates using T2-A24 cells. Stabilization efficiency was rated by mean fluorescence intensity (MFI) increase, which was calculated as MFI increase = (MFI with the given peptide – MFI without peptide)/(MFI without peptide).

(2 ≤ MFI increase < 3), low in six (1 ≤ MFI increase < 2) and not binder in one peptide (MFI increase < 1). The CMVpp65 HLA-A24-binding peptide with high BIMAS score showed high efficiency for MHC stabilization, while CEA HLA-A24-binding peptides with a BIMAS score above 100 did not always indicate high stabilization efficiency (Fig. 1).

CTL induction assay using CEA HLA-A24 peptides and serum CEA-positive cancer patient-derived PBMC. In Figure 2, six representative cases of positive CTL response are shown. These CTL responded to various CEA HLA-A24-binding peptides including peptides 3, 6, 8 and 9. Especially, CTL from Case015 demonstrated very large amounts of IFN-γ production, 9.7 ng/mL. A summary of CTL induction assays using cancer patient PBMC is shown in Table 2. The CTL derived from 29 cases responded to all CEA HLA-A24 peptides except peptides 2, 7 and 10. The frequency of positive responses was relatively high against CEA peptides 6 and 9. Among 29 cases, 12 patients including two who showed positive responses for more than two peptides, demonstrated significant IFN-γ responses against peptide-pulsed TISI cells (positive rate 41.4%). On the other hand, the positive response rate against CMVpp65 peptide as positive control was 55.2%.

Docking simulation assay for CEA HLA-A24-peptides binding to HLA protein. Eight CEA peptides and CMVpp65 were shown positive for docking simulation to HLA-A24 protein (Fig. 3). The peptide with highest affinity was CEA A24-3 (ΔG = −43.5 kJ/mol), but CEA 7 and 10 were not binding. Meanwhile, CMVpp65 A24 peptide showed high affinity (−32.2 kJ/mol).

Additionally, we prepared an example figure of our *in silico* docking simulation assay using $CMVpp65_{341–349}$ peptide, which showed a high docking affinity (Fig. 4).

Characterization of known HLA-A24-restricted peptides using various peptide-evaluation tools. Sixteen HLA-A24-restricted peptides including CMVpp65 and CEA HLA-A24 peptides 2, 6, 9 and 10 were investigated in binding activity using BIMAS,

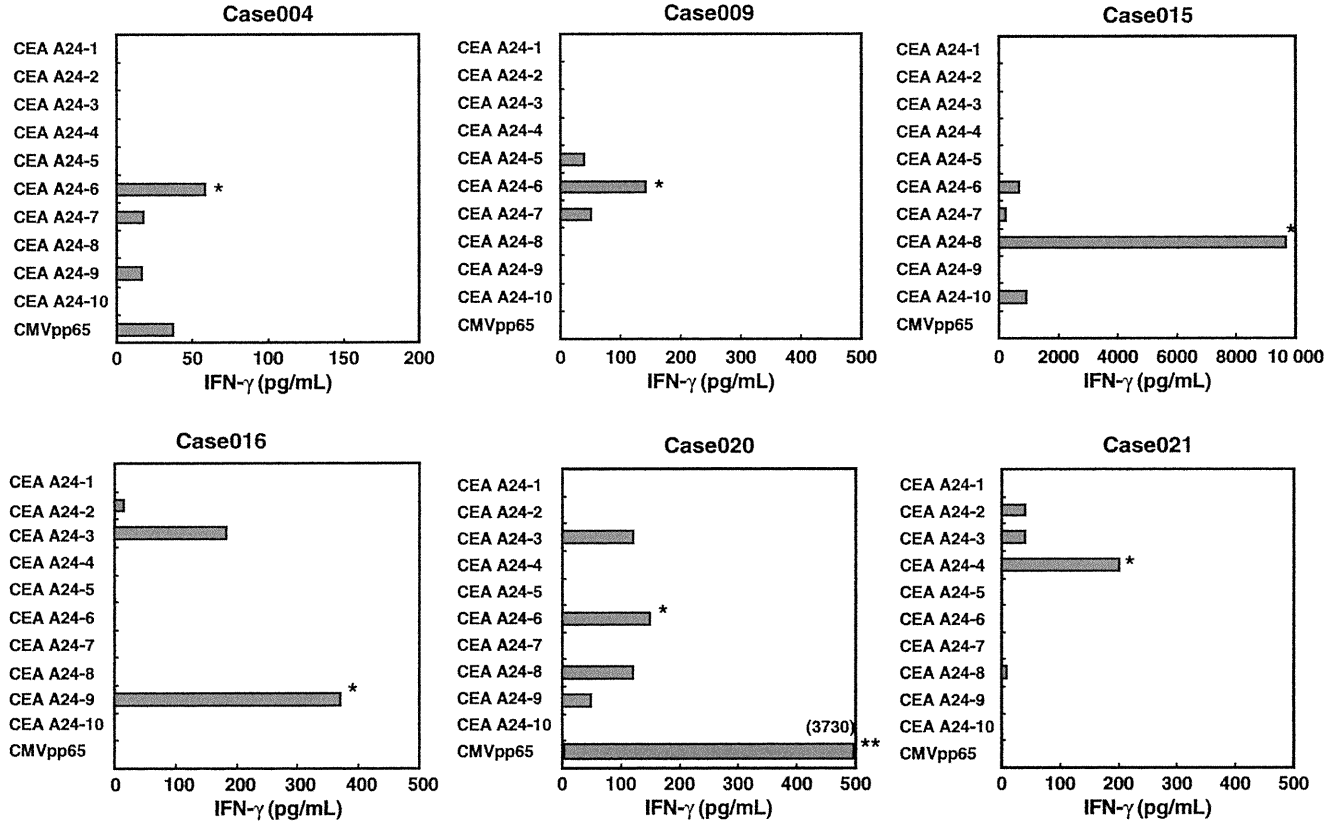

Fig. 2. The CTL inducing activity of CEA HLA-A24-restricted peptides. CTL induction cultures were successful in 29 of 32 cases of CEA-positive cancer patients. Six representative cases of positive CTL response against CEA peptides 4, 6, 8 and 9 are shown. Measuring IFN-γ levels in supernatant from co-culture of $CD8^+$ T cells and peptide-pulsed TISI cells was performed in triplicate. *$P < 0.05$, **$P < 0.01$.

doi: 10.1111/j.1349-7006.2011.01866.x

Table 2. Frequency of positive CTL-inducing activities in CEA-positive cancer patients

Peptide name	Tested cases	Positive cases	Positive rate (%)
CMVpp65 A24	29	16	55.2
CEA A24-1	29	2	6.9
CEA A24-2	29	0	0
CEA A24-3	29	1	3.4
CEA A24-4	29	2	6.9
CEA A24-5	29	2	6.9
CEA A24-6	25	4	16
CEA A24-7	29	0	0
CEA A24-8	29	1	3.4
CEA A24-9	29	3	10.3
CEA-A24-10	29	0	0
SUM	29	12†	41.4

†Two cases showed positive CTL responses for more than 2 peptides.

MHC-stabilization, docking simulation and IFN-γ production assay (Table 3). The IFN-γ production assay was performed using PBMC from enrolled HLA-*A*2402*$^{+}$ cancer patients who were not included in the CEA peptide-CTL induction cultures. BIMAS scores ranged 0.1–720. The MHC stabilization assay demonstrated that peptides with high, medium and low affinity were 5, 5 and 4, respectively. Docking simulation assay revealed that MAGE3, tyrosinase and HER2 peptides showed high affinities (<−14 kJ/mol) besides CEA and CMVpp65 peptides. The IFN-γ production assay indicated that six HLA-A24 peptides exhibited significant CTL induction activity. Taking these observations into consideration, three peptides (MAGE3, HER2-2, CMVpp65) alone showed a high score in all three parameters except BIMAS.

Correlation between peptide docking and other immunological parameters. Correlations between HLA-A24-restricted peptide docking and other immunological parameters including BIMAS, MHC stabilization and IFN-γ production, were evaluated using a correlation analysis. The MHC stabilization score was inversely correlated with the affinity calculated in docking simulation alone ($r = -0.589$, $P = 0.015$), not with BIMAS or IFN-γ production index (Fig. 5). On the other hand, BIMAS was not significantly correlated with any other parameters.

Discussion

HLA molecules are cell surface proteins that bind to antigen peptides and present them as HLA–peptide complexes to T-lymphocytes, thereby inducing a specific immune response. The binding site of HLA-class I molecules is formed by a deep cleft between two α-helices on top of an extended β-sheet structure. Only approximately bound peptides with a high affinity could trigger a potent immune response. Therefore, to identify possible high-affinity peptides derived from tumor antigens is a very important theme for developing cancer vaccines that have therapeutic efficacy.

Recently, a large amount of data for crystal structures of HLA–peptide complexes has been accumulated, allowing bioinformaticians to predict molecular binding simulations.[20,21]

Fig. 4. Docking structure of CMVpp65$_{341–349}$ peptide and HLA-A24 protein. The two subunits of HLA-A24 protein (shown as ribbons in green and cyan) are identical to chains D and F of 2BCK in the Protein Data Bank, respectively, and the CMVpp65 peptide (shown as a space-filling model of atoms) was docked to the binding pocket of the HLA protein. This model was drawn by PyMOL (http://www.pymol.org/).

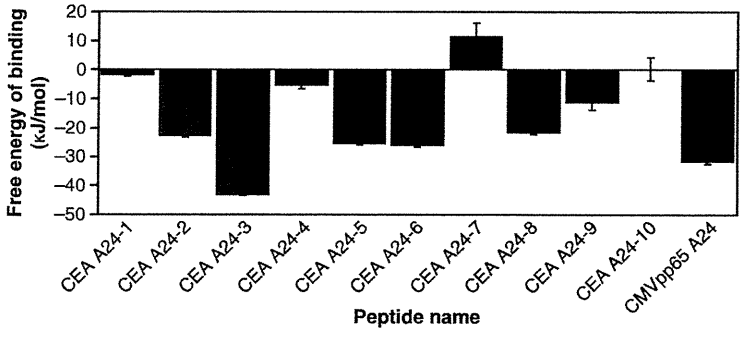

Fig. 3. Characterization of CEA HLA-A24-restricted peptides using peptide-HLA docking simulation assay. For each of 9-mer epitope candidate peptides, the mean and standard deviation of the three lowest binding free energies are shown.

Table 3. Peptide-HLA docking scores and other immunological factors of various HLA-A24-binding peptides

Peptide name	Amino acid sequence	Position	BIMAS score	MHC stabilization assay	Docking (kJ/mol)	IFN-γ production index
HIVgp120	RYLRDQQLL	584–592	720	1.60	13.5	1.02
MAGE1	NYKHCFPEI	135–143	66	3.38	−0.7	1.37
MAGE2	EYLQLVFGI	156–164	90	2.27	−6.1	1.14
MAGE3	IMPKAGLLI	195–203	1.5	3.12	−14.9	4.72
Tyrosinase	AFLPWHRLF	206–214	18	2.50	−17.3	0.96
WT1-1M	CYTWNQMNL†	235–243	200	2.87	−9.2	0.83
WT1-2	CMTWNQMNL	235–243	4	1.07	−8.4	0.97
HER2-1	TYLPTNASL	63–71	360	3.23	−14.5	0.89
HER2-2	PYVSRLLGI	780–788	7.5	3.20	−15.9	2.54
EBNA3A	RYSIFFDYM	246–254	60	1.40	−11.4	1.28
CEA A24-2	TYACFVSNL	652–660	200	2.85	−22.7	0.94
CEA A24-6	LYGPDTPII	590–598	60	2.46	−26.4	1.03
CEA A24-9	TFQQSTQEL	276–284	39.6	1.00	−11.5	2.25
CEA A24-10	KTITVSAEL	492–500	18.5	0.01	0.2	0.97
CMVpp65	QYDPVAALF	341–349	168	3.45	−32.0	2.31
gp100	VWKTWGQYW	152–160	0.1	0.34	13.1	1.00

†Modified peptide from natural $WT1_{235-243}$ peptide.

(a)

Analysis	Correlation coefficient (*r*)	*P* value
BIMAS vs MHC	0.141	0.609
BIMAS vs docking	0.274	0.311
BIMAS vs IFN-γ	0.258	0.342
MHC vs docking	−0.589	0.015* (*P* < 0.05)
MHC vs IFN-γ	0.312	0.244
Docking vs IFN-γ	−0.263	0.332

(b)

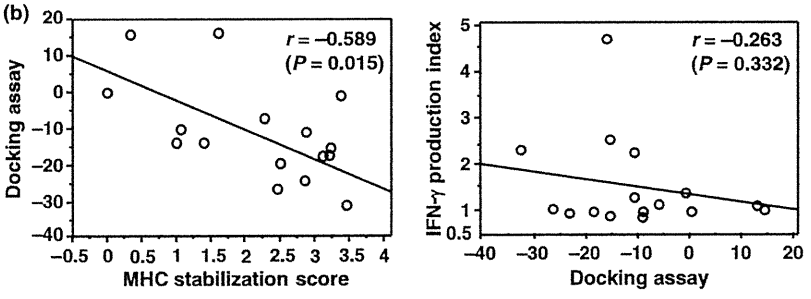

Fig. 5. Correlation of peptide–HLA binding predictions with immunological parameters. (a) Correlation of BIMAS score and peptide–HLA binding affinity predicted in docking simulation assay with MFI increase ratio in MHC stabilization assay and IFN-γ production index. MHC: MHC stabilization assay ratio; docking: peptide-HLA docking simulation assay; IFN-γ: IFN-γ production index. (b) Correlation of binding affinity predicted in docking simulation assay with MHC stabilization assay ratio or IFN-γ production index.

However, despite biophysical and biochemical analysis of HLA complexes, accurate prediction of antigen peptide binding to HLA molecule is still difficult.

In the present study, we developed an *in silico* docking simulation assay between the HLA-A24 molecule and an antigen peptide based on computational structural analysis, aiming to predict optimal docking peptides with high affinity leading to effective CTL activation. Conventional algorithms based on primary amino acid sequence have been successful so far in predicting antigenic peptides binding to the HLA class I pocket, but such algorithms have limited accuracy and provide no structural information.[22,23]

Recently, the development of algorithms to predict the structure of MHC–peptide complex has been tried. Briefly, Logean and Rognan[24] used a binding free energy scoring function in a newly developed EpiDock, and Desmet *et al.*[25] developed a quantitative structure-based affinity scoring method for prediction of anchoring peptide side chains in peptide–HLA complex.

Unfortunately, these methods have not been applied to the intact HLA-A24 protein because of no such available structure in PDB at that time. We performed, for the first time, the epitope prediction for HLA-A24 protein using the 3D complex structure of the protein and epitope (PDB code 2BCK). In this study, we applied two software packages, AutoDock and MODELLER, to a novel *in silico* assay system of peptide binding affinity. MODELLER was performed to build the initial conformation of any given peptide, and AutoDock was used to assess the affinity (ΔG) between HLA-A24 protein and the given peptide. In general, AutoDock is originally available for predicting the binding mode of low-molecular compounds in the context of receptor–ligand docking, and is not always suitable for highly flexible ligands such as 9-mer peptides. In the case of HLA–peptide docking, however, the binding pocket and epitope conformation have been well investigated, and the conformation search parameters in simulation can be limited or narrowed down differently from so called "blind docking." We have shown that a local search simulation around the binding pocket of HLA-A24

doi: 10.1111/j.1349-7006.2011.01866.x

protein reproduced the affinities between the protein and A24-restricted peptides. More importantly, all of these procedures are performed by combination of free software (AutoDock and MODELLER), suggesting that our *in silico* simulation assay is easily available to many bioinformaticians with the same interests. Recently, Fuhrmann *et al.*[26] reported a receptor–ligand docking simulation method based on a new Lamarckian genetic algorithm which can treat a large number of degrees of freedom.[26] Thus, the further improvement of an *in silico* binding assay system may be possible for not only HLA class I epitope peptides (approximately 10-mer) but also class II epitope peptides (approximately 20-mer). Additionally, we have performed MHC stabilization and CTL induction assays regarding various CEA and other HLA-A24-restricted peptides and investigated the correlation of docking simulation assay with other immunological parameters, the MHC stabilization score and IFN-γ production index.

Cytotoxic T-lymphocyte induction experiments using PBMC from CEA-positive cancer patients demonstrated that CEA A24-6 and 9 were mainly positive for CTL inducing activity. These peptides were shown to have moderate to high affinity in a docking simulation assay. These observations may support the negative selection theory that intermediate binders can be sometimes good CTL inducers in cancer patients because CTL precursors responding to high affinity peptides have been depleted in the thymus by negative selection, and such CTL may be exhausted after exposure to specific cancer antigen peptides.[27]

Unfortunately, CEA A24-3, which has the highest affinity in a docking assay, did not show strong CTL activation. Similarly, CEA A24-1, with the highest affinity in MHC stabilization, showed marginal binding score in a docking simulation, which indicates the discrepancy of affinity between docking simulations and other immunological binding assays. In our current method, unlike peptide epitopes, we did not permit the flexibility of the epitope-binding pocket structure of the HLA protein because of long computational time. The MHC stability assay suggests that CEA A24-1 is a good binder (Fig. 1), but its docking affinity is not high (Fig. 3). Since CEA A24-1 is the second largest peptide (1082.2 Da) among those in Table 1, it might not stably occupy a rigid binding pocket of HLA-A24 protein in a docking simulation. Actually, CEA A24-7, the largest peptide (1136.2 Da), has shown the lowest docking affinity. Although a strong correlation was not observed between the epitope's molecular weight and docking affinity ($r^2 = 0.16$), the rigid pocket simulation condition for HLA protein may have affected the docking conformation and affinity. A docking simulation that allows a pocket structure to be flexible is a challenge for the future, and it may be solved by advances in computer technology.

Most interestingly, CEA_{652} peptide, which is well known for specific CTL epitopes, did not show any positive CTL inducing activity in all patient PBMC. On the other hand, CEA A24-6, which showed the highest frequency of CTL induction, has not been reported as a CTL epitope previously, but few CTL induction studies using CEA-positive cancer patient PBMC have been done. Therefore, there might be some difference in CTL culture environments including immunological regulation between healthy donor and cancer patients, resulting in selection of antigenic peptides. Crosti *et al.*[7] showed four CEA helper epitopes stimulating the proliferation of $CD4^+$ T-lymphocytes from end-stage lung cancer patients. These results supported positively our results that CTL inducing activity for any CEA peptides with HLA-A24 restriction was seen in 12 of 29 cancer patients.

Nukaya *et al.*[9] reported CEA_{652}-A24-restricted peptide using healthy donor PBMC-based CTL induction assay for the first time and demonstrated peptide-stimulated CTL efficiently killed CEA-positive cancer cell lines. The CEA_{652} peptide has been also used for DC-based cancer vaccine against CEA-positive gastrointestinal solid cancers. The clinical trial by Matsuda *et al.*[10] using CEA-peptide treated DC vaccine showed that no significant clinical responses were seen, but four of seven patients developed *in vitro* CTL response against CEA peptide after vaccination. In the present study 44% of cancer patients demonstrated CTL activity against various CEA peptides; however, there was no response to CEA_{652} peptide.

In another CTL induction assay using patient PBMC and 16 well-known HLA-A24 peptides including CEA peptides, six peptides were positive for specific CTL activation. With regard to these 16 peptides, we also obtained other immunological data. In Figure 5, correlations between HLA-A24 peptide docking simulation and other immunological parameters, including BIMAS, MHC stabilization and IFN-γ production, were investigated using a correlation analysis. The binding affinity predicted in docking simulation was inversely correlated with MHC stabilization score ($r = -0.589$, $P = 0.015$), whereas BIMAS was not significantly correlated with that or any other parameter. These observations suggested that our docking simulation assay might have potential advantage in efficiency of epitope prediction over BIMAS. However, our docking simulation assay is still not developed enough to compare with other predictive programs precisely, and the accumulation of more simulation data is needed.

Recently, novel conventional algorithms based on primary amino acid sequence like BIMAS have been developed. They show better prediction than BIMAS,[28–30] but such algorithms have limited accuracy. Similarly, our *in silico* assay system has yet to predict genuine CTL epitope peptides with high affinity. Computational methods for modeling of peptide-HLA binding include threading, molecular dynamics and approaches based on HLA binding pocket recognition. Technical improvements for all methods should be requested to elevate the accuracy of CTL epitope prediction in future.

Acknowledgments

We thank Dr. Mochizuki for supplying several synthetic peptides and for excellent technical assistance. This work was supported in part by a grant from the Cooperation of Innovative Technology and Advanced Research in Evolutional Area (CITY AREA) program from the Ministry of Education, Culture, Sports, Science and Technology, Japan.

Disclosure Statement

The authors have no conflict of interest.

Abbreviations

CEA	carcinoembryonic antigen
HLA	human leukocyte antigen
PDB	The Protein Data Bank
CTL	cytotoxic T cells
BIMAS	bioinformatics and molecular analysis section
PBMC	peripheral blood mononuclear cells
CMV	cytomegalovirus

References

1 Onizawa S, Watanabe S, Yagura T, Yasutomi M, Yamamura Y. Radioimmunoassay of carcinoembryonic antigen and clinical significance of its level in plasma. *Gann* 1976; **67**: 371–8.
2 Tsai HL, Chu KS, Huang YH *et al.* Predictive factors of early relapse in UICC stage I–III colorectal cancer patients after curative resection. *J Surg Oncol* 2009; **100**: 736–43.
3 Jokerst JV, Raamanathan A, Christodoulides N *et al.* Nano-bio-chips for high performance multiplexed protein detection: determinations of cancer biomarkers in serum and saliva using quantum dot bioconjugate labels. *Biosens Bioelectron* 2009; **24**: 3622–9.

4 Kawashima I, Hudson SJ, Tsai V *et al.* The multi-epitope approach for immunotherapy for cancer: identification of several CTL epitopes from various tumor-associated antigens expressed on solid epithelial tumors. *Hum Immunol* 1998; **59**: 1–14.
5 Kavanagh B, Ko A, Venook A *et al.* Vaccination of metastatic colorectal cancer patients with matured dendritic cells loaded with multiple major histocompatibility complex class I peptides. *J Immunother* 2007; **30**: 762–72.
6 Pickford WJ, Watson AJ, Barker RN. Different forms of helper tolerance to carcinoembryonic antigen: ignorance and regulation. *Clin Cancer Res* 2007; **13**: 4528–37.
7 Crosti M, Longhi R, Consogbo G, Melloni G, Zannini P, Protti MP. Identification of novel subdominant epitopes on the carcinoembryonic antigen recognized by CD4 $^{+}$ T cells of lung cancer patients. *J Immunol* 2006; **176**: 5093–9.
8 Iero M, Squarcina P, Romero P *et al.* Low TCR avidity and lack of tumor cell recognition in CD8(+) T cells primed with the CEA-analogue CAP1-6D peptide. *Cancer Immunol Immunother* 2007; **56**: 1979–91.
9 Nukaya I, Yasumoto M, Iwasaki T *et al.* Identification of HLA-A24 epitope peptides of carcinoembryonic antigen which induce tumor-reactive cytotoxic T lymphocyte. *Int J Cancer* 1999; **80**: 92–7.
10 Matsuda K, Tsunoda T, Tanaka H *et al.* Enhancement of cytotoxic T-lymphocyte responses in patients with gastrointestinal malignancies following vaccination with CEA peptide-pulsed dendritic cells. *Cancer Immunol Immunother* 2004; **53**: 609–16.
11 Itoh T, Ueda Y, Kawashima I *et al.* Immunotherapy of solid cancer using dendritic cells pulsed with the HLA-A24-restricted peptide of carcinoembryonic antigen. *Cancer Immunol Immunother* 2002; **51**: 99–106.
12 Ueda Y, Itoh T, Nukaya I *et al.* Dendritic cell-based immunotherapy of cancer with carcinoembryonic antigen-derived, HLA-A24-restricted CTL epitope: clinical outcomes of 18 patients with metastatic gastrointestinal or lung adenocarcinomas. *Int J Oncol* 2004; **24**: 909–17.
13 Ojima T, Iwahashi M, Nakamura M *et al.* Streptococcal preparation OK-432 promotes the capacity of dendritic cells (DCs) to prime carcinoembryonic antigen (CEA)-specific cytotoxic T lymphocyte responses induced with genetically modified DCs that express CEA. *Int J Oncol* 2008; **32**: 459–66.
14 Sali A, Blundell TL. Comparative protein modelling by satisfaction of spatial restraints. *J Mol Biol* 1993; **234**: 779–815.
15 Morris GM, Goodsell DS, Halliday RS *et al.* Automated docking using a Lamarckian genetic algorithm and an empirical binding free energy function. *J Comput Chem* 1998; **19**: 1639–62.
16 Berman HM, Battistuz T, Bhat TN *et al.* The Protein Data Bank. *Acta Crystallogr D Biol Crystallogr* 2002; **58**: 899–907.
17 Knorr R, Trzeciak A, Bannwarth W, Gillessen D. New coupling reagents in peptide chemistry. *Tetrahedron Lett* 1989; **30**: 1927–30.
18 Kuzushima K, Hayashi N, Kimura H, Tsurumi T. Efficient identification of HLA-A*2402-restricted cytomegalovirus-specific CD8(+) T-cell epitopes by a computer algorithm and an enzyme-linked immunospot assay. *Blood* 2001; **98**: 1872–81.
19 Abbas AK, Lichtman AH, Pillai S. The major histocompatibility complex. In: Abbas AK, Lichtman AH, Pillai S, eds. *Cellular and Molecular Immunology*, 6th edn. Philadelphia: Saunders, 2010; 97–111.
20 Sieker F, May A, Zacharias M. Predicting affinity and specificity of antigenic peptide binding to major histocompatibility class I molecules. *Curr Protein Pept Sci* 2009; **10**: 286–96.
21 Schiewe AJ, Hawworth IS. Structure-based prediction of MHC-peptide association: algorithm comparison and application to cancer vaccine design. *J Mol Graph Model* 2007; **26**: 667–75.
22 Shastri N. Needles in haystacks: identifying specific peptide antigens for T cells. *Curr Opin Immunol* 1996; **8**: 271–7.
23 Pelte C, Cherepnev G, Wang Y, Schoenemann C, Volk HD, Kern F. Random screening of proteins for HLA-A*0201-binding nine-amino acid peptides is not sufficient for identifying CD8 T cell epitopes recognized in the context of HLA-A*0201. *J Immunol* 2004; **172**: 6783–9.
24 Logean A, Rognan D. Recovery of known T-cell epitopes by computational scanning of a viral genome. *J Comput Aided Mol Des* 2002; **16**: 229–43.
25 Desmet J, Meersseman G, Boutonnet N *et al.* Anchor profiles of HLA-specific peptides: analysis by a novel affinity scoring method and experimental validation. *Proteins* 2005; **58**: 53–69.
26 Fuhrmann J, Rurainski A, Lenhof HP, Neumann D. A new Lamarckian genetic algorithm for flexible ligand-receptor docking. *J Comput Chem* 2010; **31**: 1911–8.
27 Kazansky DB. Intrathymic selection: new insight into tumor immunology. *Adv Exp Med Biol* 2007; **601**: 133–44.
28 Bui HH, Schiewe AJ, von Grafenstein H, Haworth LS. Structural prediction of peptides binding to MHC class I molecules. *Proteins* 2006; **63**: 43–52.
29 Rammensee HG, Bachmann J, Emmerich NN, Bachor OA, Stevanovic S. SYFPEITHI: database for MHC ligands and peptides motifs. *Immunogenetics* 1999; **50**: 213–9.
30 Buus S, Lauemoller SL, Worning P *et al.* Sensitive quantitative predictions of peptide-MHC binding by a 'Query by Committee' artificial neural network approach. *Tissue Antigens* 2003; **62**: 378–84.

doi: 10.1111/j.1349-7006.2011.01866.x

Gen Thorac Cardiovasc Surg (2011) 59:579–582
DOI 10.1007/s11748-010-0733-5

CASE REPORT

Disseminated calcifying tumor of the pleura: review of the literature and a case report with immunohistochemical study of its histogenesis

Mitsuhiro Isaka, MD · Kazuo Nakagawa, MD
Tomohiro Maniwa, MD · Shinsuke Saisho, MD
Yasuhisa Ohde, MD · Takehiro Okumura, MD
Haruhiko Kondo, MD · Takashi Nakajima, MD

Received: 30 April 2010 / Accepted: 21 September 2010

Abstract Calcifying tumor of the pleura is a rare benign tumor, similar to the calcifying fibrous pseudotumor originally described in the subcutaneous and deep soft tissues of the extremities, trunk, and neck. Calcifying tumors of the pleura have also been reported infrequently as disseminated lesions. Here we report a case of disseminated calcifying tumor of the pleura, with some new findings obtained in this study, and review the literature of disseminated calcifying tumor of the pleura.

Key words Calcifying tumor · Calcifying fibrous pseudotumor · Pleura dissemination · Osteopontin

Introduction

In 1993, Fetch et al. first described a calcifying fibrous pseudotumor as a benign soft tissue tumor characterized by the presence of dense collagenization with psammomatous calcification and lymphoplasmacytic cell infiltrates.[1] Later, similar tumors were reported in the pleura and were termed calcifying fibrous tumor or pseudotumor. In the newly published *Classification of Tumours of the Lung, Pleura, Thymus and Heart* by the World Health Organization, this lesion has been designated "calcifying tumor of the pleura" (CTP), which is synonymous with the previous calcifying fibrous pseudotumor.[2] Moreover, CTP have been reported as disseminated multiple lesions in the pleura.[3–7] Herein we present an additional disseminated CTP case with new immunohistochemical findings accompanied by a literature review.

M. Isaka (✉) · K. Nakagawa · T. Maniwa · S. Saisho · Y. Ohde · T. Okumura · H. Kondo
Division of Thoracic Surgery, Shizuoka Cancer Center, 1007 Shimonagakubo, Nagaizumi-cho, Sunto-gun, Shizuoka 411-8777, Japan
Tel. +81-55-989-5222; Fax +81-55-989-5634
e-mail: mi.isaka@scchr.jp

T. Nakajima
Division of Diagnostic Pathology, Shizuoka Cancer Center, Shizuoka, Japan

Case report

A 40-year-old Japanese man was referred to our hospital for further evaluation of a pleural mass initially found by a computed tomography (CT) scan of his chest. He had felt an uncomfortable feeling in his back. He had no history of smoking or asbestos exposure. A CT scan revealed a wide mass, 75 mm in maximum diameter, on the chest wall in the right dorsal area (Fig. 1). The mass appeared as diffuse high-density areas in the scan. Using integrated ^{18}F-fluorodeoxyglucose positron emission tomography (FDG-PET)/CT imaging, the maximum standardized uptake (SUV_{max}) value of this mass was found to be 2.0, which was too low to consider the tumor as malignant. Percutaneous needle biopsy was performed, and the histological diagnosis was suggestive of CTP. Because the patient refused surgical treatment at first, he was carefully followed with CT scans for more than 2 years, but tumor size was unchanged. Finally, video-assisted surgery through a mini-thoracotomy was performed to remove the tumor.

At surgery, the largest tumor, 6.8 cm in diameter, was found to be suspended from two long pedicles and hanging down into the thoracic cavity from the chest

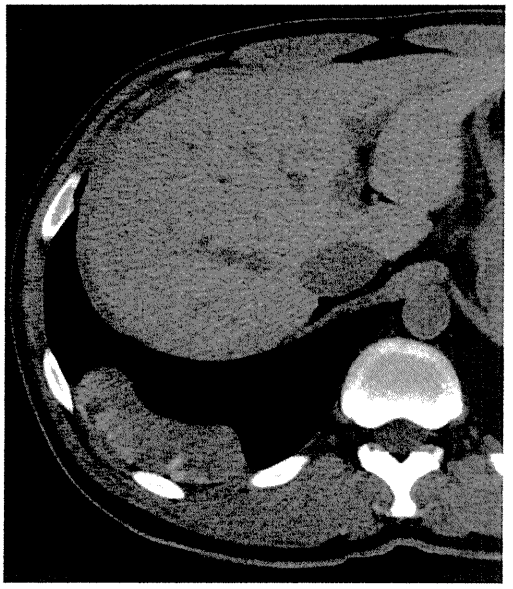

Fig. 1 Computed tomography (CT) scan image. A subpleural mass was seen in the posterior part of the lower part of the right lung

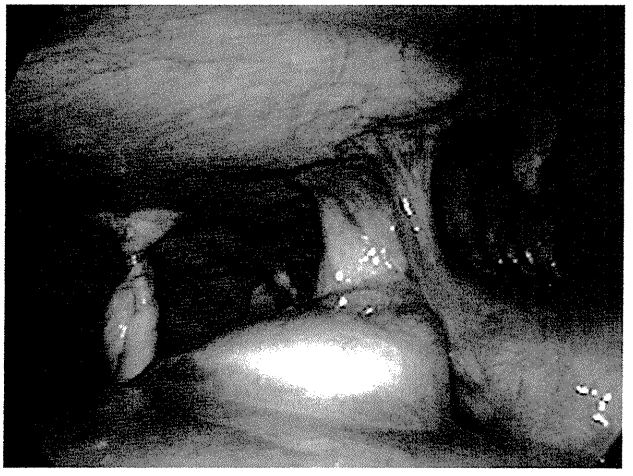

Fig. 2 Thoracoscopic view of disseminated calcifying tumor of the pleura (CTP). The largest tumor was found suspended with a long pedicle into the thoracic cavity from the chest wall. Another small tumor was also found hanging down beside the main tumor

wall (Fig. 2). Two other tumors, 2.0 cm in diameter, were also suspended from pedicles similar to the largest tumor. Many additional small nodules were present on the diaphragm, especially in the fatty tissue of the costophrenic angle. We resected all 17 visible lesions. The largest mass had a shiny surface and was lobulated in shape. All the lesions were firm, well circumscribed, but unencapsulated, and ash gray in color at the cut surface. The smallest nodule was about 2 mm in diameter.

The diagnosis was confirmed by histopathology using hematoxylin and eosin staining. Histologically, the central part of the larger tumors consisted of paucicellular, dense collagenous tissue with many psammomatous dystrophic calcifications. The peripheral areas of the largest tumor and many of the small tumors were composed of fibrogranulomatous tissue with plasma cell infiltrations and vascular proliferation. Moreover, there were many spindle-shaped or stellate fibroblast-like cells with large nuclei and abundant pale cytoplasm, sometimes forming multinucleated giant cells (Fig. 3a). Immunohistochemically, these cells were positive for vimentin and osteopontin, but negative for AE1/AE3, epithelial membrane antigen (EMA), desmin, HHF35, α-smooth muscle actin (ASMA), caldesmon, and anaplastic lymphoma kinase-1 (ALK-1), CD34, and CD68 (Fig. 3b). Osteopontin immunostaining was strongly positive for the psammoma bodies and many CD68-positive histiocytes (Fig. 3c,d).

The patient's postoperative course was uneventful, and no evidence of local recurrence or distant metastasis was found at 28 months after surgery.

Discussion

The previously reported cases of disseminated CTP and our case are summarized in Table 1.[3–7] Mean age was 35.7 years (range, 23–52 years); there were two men and four women. Half these CTP cases, including our case, were reported from Japan. Most disseminated CTP is asymptomatic and found incidentally on radiographs. CT images of these tumors have been reported, but FDG-PET/CT images have not been previously reported. Our FDG-PET image revealed a very low SUV_{max} value, which suggested a benign lesion. With regard to its prognosis, no disease-related death has been reported for disseminated CTP, although its local recurrence has been observed.[1,8,9] The disseminated CTP might be benign rather than malignant given the radiologic and clinical findings. Previous reports and our immunohistochemical study revealed that the spindle-shaped fibroblastic cells in CTP were positive for vimentin and negative for cytokeratin, EMA, ASMA, desmin, S-100 protein, CD34, and ALK-1. Although these findings do not clarify the histogenesis of this tumor, CTP might differ from benign spindle cell tumors such as solitary fibrous tumors and inflammatory myofibroblastic tumors.[8–10]

We first studied immunohistochemical osteopontin expression in this CTP and found that the CTP was composed mainly of spindle-shaped or stellate cells, which were immunohistochemically positive for osteo-

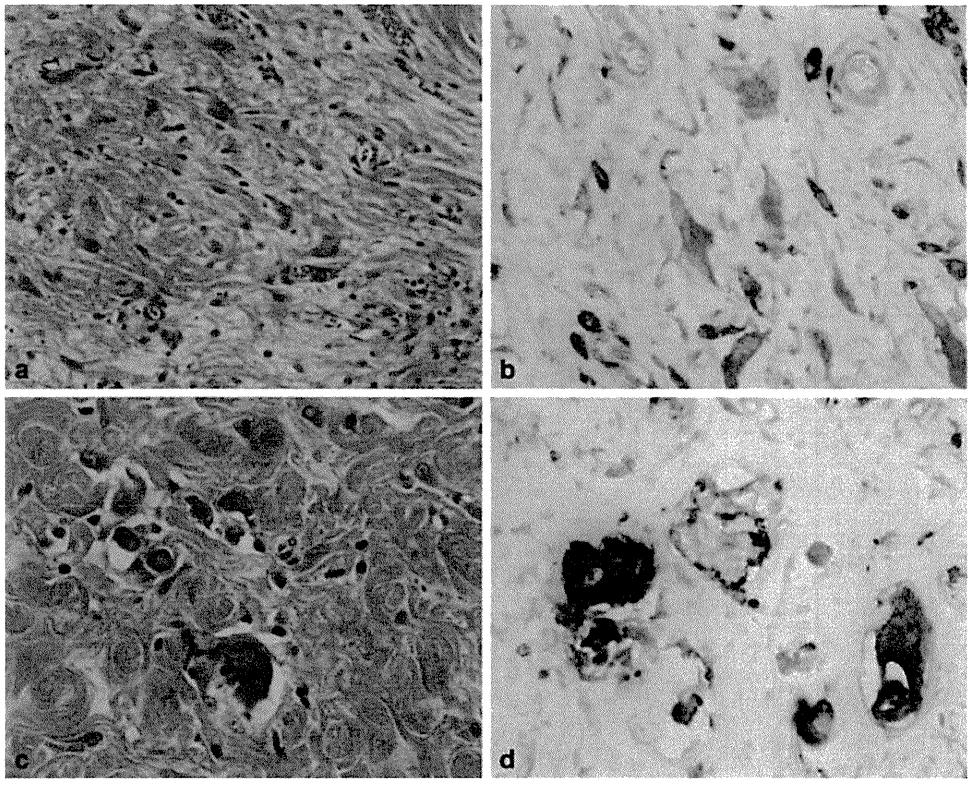

Fig. 3 Histopathological findings of disseminated CTP. **a** In the peripheral area of the tumor, the fibrous tissue contained inflammatory cells and large fibroblastic cells with pale cytoplasm. **b** Double immunohistochemistry showed that large fibroblastic cells were positive for only osteopontin (*brown*) and that histiocytic cells were positive for both osteopontin and CD68 (*dark blue*). **c** Psammomatous calcification was usually seen in the dense fibrous tissue in the central area of the tumor, sometimes closely associated with inflammatory cells such as histiocytes and plasma cells. **d** Double immunohistochemistry showed that psammomatous calcifications were positive for osteopontin (*brown*), and large histiocytic cells (*blue-brown*) positive for both osteopontin and CD68 were present adjacent to the psammomatous calcifications

pontin. There are two types of osteopontin-positive cells: osteopontin-positive but CD68-negative fibroblast-like cells and osteopontin-positive and CD68-positive histiocytes. Osteopontin is a cytokine that is associated with inflammation and tissue remodeling.[11,12] Signals mediated by inflammatory cells such as macrophages and neutrophils trigger expression of osteopontin in fibroblasts, which correlates with collagen production.[11] It is possible that the osteopontin-positive cells were fibroblasts leading to collagen deposition in the CTP. Moreover, psammoma bodies were strongly positive for osteopontin and sometimes were closely associated with CD68-positive histiocytes in our case. Osteopontin is also produced by macrophages and stimulates other macrophages.[13] These macrophages are effector cells controlling ectopic calcification,[14] and osteopontin plays a significant role in the development of psammoma bodies.[15] These findings may suggest that the CPT is not a true neoplasm, and that the multifocal and recurrent lesions appear during unusual inflammatory-reparative processes mediated by osteopontin expression. Osteopontin expression might be associated with the pathogenesis of disseminated CTP. Further studies are necessary, including clonality analysis of this tumor.

We followed up this case of disseminated CTP before and after surgery for the longest time reported to date. Although the long-term prognosis for patients with CTP is unclear, several studies have demonstrated that their clinical courses are good, even if they have disseminated lesions. Complete resection with a margin of normal tissue appears optimal, and should reduce the possibility of local recurrences, even among disseminated CTP. It is still unclear whether this treatment strategy is essential for patients with disseminated CTP. More knowledge about this is required to handle surprising disseminated lesions.

Table 1 Previously reported cases of disseminated calcifying tumors of the pleura

Case	First author (year) and country	Age/sex	Diagnostic procedure	Operation	Time before surgery	Follow-up (months)	Recurrence	Immunostaining positive	Immunostaining negative
1	Pinkard (1996) USA	23/F	Surgical specimen	Resection of all lesions	–	9	None	NR	NR
2	Hainaut (1999) Belgium	29/F	Surgical specimen	Resection of only the main tumor	–	NR	Alive with disease	NR	NR
3	Kawahara (2005) Japan	35/F	Surgical specimen	Resection of all lesions	2 years	NR	NR	Vimentin, factor XIIIa	SMA, CD34, S-100, desmin, AE-1/AE-3, ALK
4	Shibata (2008) Japan	52/F	Needle biopsy	Resection of only the main tumor	–	4	Alive with disease	Vimentin	CD34, factor XIIIa, SMA, desmin, CD68, beta-cell CLL/lymphoma 2
5	Suh (2008) Korea	35/M	Surgical specimen	Resection of all lesions	–	16	None	Vimentin, SMA, CD34	desmin, ALK
6	Present case Japan	40/M	Needle biopsy	Resection of all lesions	2 years	28	None	Osteopontin, vimentin, CD68	CD34, S-100, AE-1/AE-3, EMA, CEA

NR, not reported; SMA, smooth muscle actin; ALK, anaplastic lymphoma kinase; CLL, chronic lymphocytic leukemia; EMA, epithelial membrane antigen; CEA, carcinoembryonic antigen

References

1. Fetsch JF, Montgomery EA, Meis JM. Calcifying fibrous pseudotumor. Am J Surg Pathol 1993;17:502–8.
2. Travis WD, Churg A, Aubry MC. Calcifying tumor of the pleura. In: Travis WD, Brambilla E, Muller-Hermelink HK, Harris CC, editors. Pathology and genetics of tumours of the lung, pleura, thymus and heart. World Health Organization classification of tumours. IARC Press: Lyon, France; 2004. p. 143–4.
3. Hainaut P, Lesage V, Weynand B, Coche E, Noirhomme P. Calcifying fibrous pseudotumor (CFPT): a patient presenting with multiple pleural lesions. Acta Clin Belg 1999;54:162–4.
4. Kawahara K, Yasukawa M, Nakagawa K, Katsura H, Nagano T, Iwasaki T. Multiple calcifying fibrous tumor of the pleura. Virchows Arch 2005;447:1007–8.
5. Pinkard NB, Wilson RW, Lawless N, Dodd LG, McAdams HP, Koss MN, et al. Calcifying fibrous pseudotumor of pleura. A report of three cases of a newly described entity involving the pleura. Am J Clin Pathol 1996;105:189–94.
6. Shibata K, Yuki D, Sakata K. Multiple calcifying fibrous pseudotumors disseminated in the pleura. Ann Thorac Surg 2008;85:e3–5.
7. Suh JH, Shin OR, Kim YH. Multiple calcifying fibrous pseudotumor of the pleura. J Thorac Oncol 2008;3:1356–8.
8. Hill KA, Gonzalez-Crussi F, Chou PM. Calcifying fibrous pseudotumor versus inflammatory myofibroblastic tumor: a histological and immunohistochemical comparison. Mod Pathol 2001;14:784–90.
9. Nascimento AF, Ruiz R, Hornick JL, Fletcher CD. Calcifying fibrous "pseudotumor": clinicopathologic study of 15 cases and analysis of its relationship to inflammatory myofibroblastic tumor. Int J Surg Pathol 2002;10:189–96.
10. Sigel JE, Smith TA, Reith JD, Goldblum JR. Immunohistochemical analysis of anaplastic lymphoma kinase expression in deep soft tissue calcifying fibrous pseudotumor: evidence of a late sclerosing stage of inflammatory myofibroblastic tumor? Ann Diagn Pathol 2001;5:10–4.
11. Kohan M, Breuer R, Berkman N. Osteopontin induces airway remodeling and lung fibroblast activation in a murine model of asthma. Am J Respir Cell Mol Biol 2009;41:290–6.
12. Mori R, Shaw TJ, Martin P. Molecular mechanisms linking wound inflammation and fibrosis: knockdown of osteopontin leads to rapid repair and reduced scarring. J Exp Med 2008;205:43–51.
13. Scatena M, Liaw L, Giachelli CM. Osteopontin: a multifunctional molecule regulating chronic inflammation and vascular disease. Arterioscler Thromb Vasc Biol 2007;27:2302–9.
14. Jahnen-Dechent W, Schafer C, Ketteler M, McKee MD. Mineral chaperones: a role for fetuin-A and osteopontin in the inhibition and regression of pathologic calcification. J Mol Med 2008;86:379–89.
15. Tunio GM, Hirota S, Nomura S, Kitamura Y. Possible relation of osteopontin to development of psammoma bodies in human papillary thyroid cancer. Arch Pathol Lab Med 1998;122:1087–90.

Gen Thorac Cardiovasc Surg (2011) 59:748–752
DOI 10.1007/s11748-011-0811-3

ORIGINAL ARTICLE

Surgical treatment for gastrointestinal metastasis of non-small-cell lung cancer after pulmonary resection

Ayako Fujiwara, MD · Jiro Okami, MD, PhD
Toshiteru Tokunaga, MD, PhD · Jun Maeda, MD, PhD
Masahiko Higashiyama, MD, PhD
Ken Kodama, MD, PhD

Received: 13 October 2010 / Accepted: 4 April 2011

Abstract
Purpose. Gastrointestinal metastasis is not common in recurrent non-small-cell lung cancer (NSCLC) patients. There is thus limited information on clinical outcome for these patients. This report presents the clinical characteristics and outcomes of patients with gastrointestinal metastasis after pulmonary resection.
Methods. The study retrospectively analyzed nine NSCLC patients with gastrointestinal metastases.
Results. Gastrointestinal metastases were observed in the small intestine ($n = 4$), colon or rectum ($n = 4$), and stomach ($n = 1$). All of the patients were symptomatic. The median survival after gastrointestinal recurrence was 10.8 months. Gastrointestinal surgery was performed in five patients, whereas no cancer treatment was indicated in the remaining four patients. Three patients who underwent surgery for a solitary metastasis survived for more than 2 years after surgery with no other recurrence.
Conclusion. Surgical resection of gastrointestinal metastasis is indicated not only for symptom relief but also for providing a potentially long-term survival if the patients are properly selected.

Key words Gastrointestinal metastasis · Non-small-cell lung cancer · Surgery

A. Fujiwara · J. Okami (✉) · T. Tokunaga · J. Maeda · M. Higashiyama · K. Kodama
Department of Thoracic Surgery, Osaka Medical Center for Cancer and Cardiovascular Diseases, 1-3-3 Nakamichi, Higashinari, Osaka 537-8511, Japan
Tel. +81-6-6972-1181; Fax +81-6-6981-8055
e-mail: okami-ji@mc.pref.osaka.jp

Introduction

Surgical resection is the most effective treatment for early-stage non-small cell lung cancer (NSCLC), and it can provide the maximum opportunity for cure and improved survival. Despite complete surgical resection, however, 50%–60% of patients with stage I–IIIA NSCLC relapse and die from their lung cancer.[1] Once the disease has recurred, it is seldom curable.[2] The most common sites of recurrence are the regional lymph nodes, lung, liver, bone, brain, and adrenal glands.[3]

The gastrointestinal tract is one of the target organs of metastatic disease in NSCLC patients. Gastrointestinal metastasis often produces serious symptoms that impair the patients' quality of life, such as intestinal obstruction, gastrointestinal discomfort, hemorrhage, and abdominal pain.[4] It also may cause life-threatening events.

The principal strategy for metastatic disease in distant organs is chemotherapy because the disease is recognized as a systemic one. The physicians often hesitate to perform chemotherapy in patients with gastrointestinal metastasis because the treatment itself may increase the risk of perforation or bleeding. Meanwhile, surgical resection can be considered to prevent such a life-threatening event. According to previous reports, locoregional therapy such as surgery and radiotherapy yield excellent outcomes as well as symptom controls in a subset of patients with brain or adrenal gland metastases.[5,6] Surgical treatment for gastrointestinal metastasis has not been well described.

This report presents the clinical characteristics and outcomes of the patients with gastrointestinal metastasis after pulmonary resection.

Patients and methods

Patients

A total of 1552 patients underwent surgical treatment for NSCLC at the Osaka Medical Center for Cancer and Cardiovascular Diseases between January 1988 and December 2007. The institutional database included clinicopathological information and the postoperative clinical course, which includes the recurrence sites. The database was examined retrospectively, and the patients who had recurrence of the disease in gastrointestinal organs were identified to select the optimal patients for this study. Patients who underwent palliative or incomplete lung surgery for intrathoracic diseases were excluded. Patients were also excluded if they had any other metastatic disease before the gastrointestinal metastasis. However, patients with other metastatic foci were included if they were found at the same time as the gastrointestinal metastases or had been well controlled before the pulmonary resection, such as solitary brain metastasis. The performance status (PS) was evaluated according to Eastern Cooperative Oncology Group (ECOG) guidelines. The primary variables were patient age, sex, symptoms, stage at the time of pulmonary resection, histology, metastatic sites, and the interval between pulmonary resection and diagnosis of gastrointestinal metastasis.

Diagnosis of gastrointestinal metastasis

Patients were typically scheduled for clinic visits at 3-month intervals for the first 2 years after surgery. Patients suspected to have gastrointestinal recurrence during the follow-up period were instructed to undergo chest/abdominal computed tomography (CT), an endoscopic examination, and a histological examination with endoscopic guidance. In addition, the patients were examined before determining the treatment strategy if they had a metastatic lesion other than in the gastrointestinal tract; they were subjected to magnetic resonance imaging (MRI) of the brain and bone scintigraphy or ^{18}F-fluorodeoxyglucose positron emission tomography (FDG-PET). The interval from the date of pulmonary resection to the date of the diagnosis of gastrointestinal recurrence was recorded. The survival time was measured from the date of the diagnosis of the gastrointestinal metastasis to the date of the most recent follow-up examination or the date of death.

Statistical analysis

The statistical analysis was performed using the StatView version 5.0 software package (Abacus Concepts, Berkeley, CA, USA). The overall survival curves were estimated using the Kaplan-Meier technique.

Results

Patient characteristics

Gastrointestinal metastasis was recorded in nine patients (0.58%). The clinical information for each patient is summarized in Table 1. Two patients with solitary brain metastasis (cases 6, 8), that were well controlled after either stereotactic radiosurgery or surgical removal, were included. One patient (case 3) received adjuvant chemotherapy after pulmonary resection.

Symptoms and diagnosis of gastrointestinal metastasis

All of the patients had gastrointestinal symptoms (Table 1). Gastrointestinal metastases were observed in the small intestine (n = 4), colon or rectum (n = 4), and stomach (n = 1). More than two metastatic tumors in gastrointestinal organs were observed simultaneously in two patients (cases 4, 7). A histological diagnosis of recurrent NSCLC was obtained by endoscopic biopsy in three patients (cases 1, 6, 7), by surgical specimens in four patients (cases 2–5), or by autopsy (cases 7, 8). In most of the patients, the histological type was large-cell carcinoma or pleomorphic carcinoma. The diagnosis was not difficult because these histological types are rare as a primary gastrointestinal malignancy. One patient (case 9) was diagnosed in a different hospital by radiological examinations and underwent treatment there. Although histological examination was not obtained for this patient, the gastrointestinal metastasis from lung cancer may be a valid diagnosis according to the report from the hospital.

Multiple metastatic diseases were detected in six patients by systematic examination, but no intrathoracic recurrences (e.g., lymph node or pulmonary metastases) were observed in any of the patients.

Treatment

Gastrointestinal surgery was performed in five patients (cases 1–5). The interval from the pulmonary resection to the gastrointestinal metastasis was 1.2–19.6 months (median 6.9 months). Surgical procedure included resection of the intestinal metastasis with immediate anastomosis in all patients. The recurrent disease was completely removed in three patients (cases 1–3) who had a solitary metastasis. No cancer treatment was indicated owing to poor performance status in three (cases 6–8) of the four

Table 1 Clinicopathological findings in nine patients with gastrointestinal metastases

No.	Age[a] sex	His.	stage	GI metastatic site	Metastasis other than GI organs	Symptoms	PS	Treatment	Interval[b] (months)	Survival[c] (months)	Outcome
1	66/F	Pleo	IIIB	Colon	None	Melena	0	Surgery	6.7	40	AWD
2	68/M	Large	IIIB	Small intestine	None	Anemia	0	Surgery	9.5	93.6	AWD
3	70/F	Por Ad	IA	Rectum	None	Melena	1	Surgery	19.5	46.9	DOC
4	48/M	Large	IIB	Small intestine	Adrenal	Melena, vomiting	2	Surgery	9.4	14.9	DOD
5	83/M	Pleo	IIB	Colon	Liver	Abdominal mass	0	Surgery	6.9	3.7	DOD
6	51/M	Large	IV	Stomach	Skin (multiple)	Anemia	3	Supportive cares	2.2	0.4	DOD
7	57/M	Pleo	IIIB	Small intestine, Stomach	Liver, Kidney	Anemia, Ileus	2	Supportive cares	1.2	1.1	DOD
8	69/M	Por Ad	IV	Colon	Adrenal, brain	Unknown	2	Supportive cares	14.3	0.2	DOD
9	70/M	Large	IB	Small intestine	Adrenal, Pancreas	Melena	0	Supportive cares	4	10.8	DOD

GI, gastrointestinal; His, histology; por, poorly differentiated; Ad, adenocarcinoma; Large, large cell carcinoma; Pleo, pleomorphic carcinoma; AWD, alive without disease; DOD, dead of disease; DOC, dead of other causes
[a]Age when GI metastasis was diagnosed
[b]Interval from pulomonary resection to GI metastasis
[c]Survival after gastrointestinal metastases

patients who did not undergo surgery, and the fourth (case 9) had multiple metastases diagnosed within a short interval after pulmonary resection.

Symptom control and survival after gastrointestinal metastasis

The median survival of all nine patients after gastrointestinal recurrence was 10.8 months. The overall survival rates at 1 and 3 years after recurrence were 44.4% and 33.3%, respectively (Fig. 1). Three patients (cases 1–3) who underwent surgery for a solitary metastasis had not developed any other metastasis after surgery for more than 2 years. Two patients (cases 4, 5) who had undergone surgery to control the symptoms associated with gastrointestinal metastasis died of the disease within a year after surgery; however, the symptoms subsided after surgery, and the patients were able to enjoy oral food intake for several months. Interestingly, no additional gastrointestinal recurrence was observed in the patients who underwent surgery for the first recurrence. In contrast, four patients who did not undergo gastrointestinal surgery died less than a year after their gastrointestinal metastases were diagnosed.

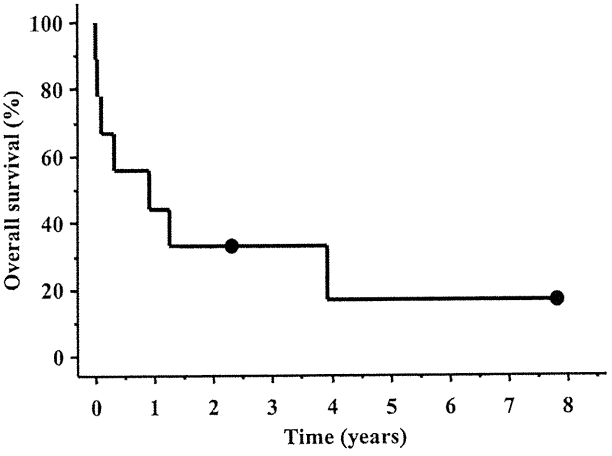

Fig. 1 Kaplan-Meier curve for the overall survival of patients with gastrointestinal metastasis from non-small-cell lung cancer

Discussion

In one study, the most common site of first recurrence was the intrathoracic lesion in 44% of recurrent NSCLC patients, the extrathoracic lesion in 44%, and combined intrathoracic and extrathoracic lesions in 12%.[7] The common extrathoracic metastatic sites are brain (32%), bone (23%), liver (9%), and adrenal gland (6%). The occurrence rate of gastrointestinal metastasis was 0.19% of all lung cancer patients[8] and 0.5% of patients who were treated surgically[9] in previous studies. Gastrointestinal metastasis is seen in only a small proportion of the population of NSCLC patients with recurrence, but it is important in clinical practice. Gastrointestinal recur-

rence may cause abdominal symptoms such as pain or distention, gastrointestinal obstruction, and bleeding, which are symptoms not usually associated with thoracic disease. Gastrointestinal metastasis from lung cancer may occur at the late or terminal stage over the course of the disease.[10] Therefore, most patients with gastrointestinal metastasis receive only palliative or supportive care.

The current study selected patients who were considered potential candidates for treatment of their gastrointestinal metastases. The occurrence rate was 0.58%. All patients were symptomatic, and the clinical symptoms due to gastrointestinal recurrence appeared within 20 months of pulmonary resection. The median interval from pulmonary resection to gastrointestinal metastasis was 6.9 months, and the median survival was 10.8 months in this study. The disease-free interval from complete resection to any kind of recurrence was reported to be 11.5 months in one study[7] and 12.2 months in another.[11] Gastrointestinal metastasis may therefore tend to develop earlier than metastases at other sites.

Gastrointestinal metastases may occur with any kind of NSCLC histology. Large-cell carcinoma and squamous cell carcinoma are relatively common.[12,13] There were three cases of pleomorphic carcinoma histology in the current series. This should be noted because pleomorphic carcinoma is a rare type of histology, being found in approximately 1.3% of all surgical patients with primary NSCLC in the database. The clinical behavior of pleomorphic carcinoma is known to be aggressive, with frequent distant metastases. Gastrointestinal organs should be taken into consideration as possible metastatic site in patients with pleomorphic carcinoma.

The most important treatment option for recurrent NSCLC is chemotherapy. Nevertheless, chemotherapy was not indicated for the gastrointestinal recurrence in any patients in this study. Chemotherapy was thought to increase the risk of gastrointestinal perforation and bleeding. In fact, a case of intestinal perforation that may have resulted from necrosis of the tumor caused by chemotherapy was described in a series of small bowel metastases from primary lung carcinoma.[14]

We considered surgery an option to manage gastrointestinal metastasis. There are two principal objectives of such surgery. One is to treat the disease, and the other is to relieve the symptoms associated with the metastasis. The clinical impact of surgical resection of a gastrointestinal metastasis has not been thoroughly discussed. Five patients underwent gastrointestinal surgery in this study. It should be emphasized that three patients are experiencing long survivals after resection without another recurrence. In addition, the gastrointestinal symptoms in the remaining two patients were well controlled after surgery. In contrast, four patients who did not undergo surgery had a shorter survival after the diagnosis of gastrointestinal metastasis. Notably, three died within only 2 months. Therefore, resection of gastrointestinal metastasis may provide benefits in terms of both symptom control and survival if the patients are properly selected.

The long-term survivors in this study had a metachronous solitary metastasis after a relatively long interval (≥6 months) between pulmonary resection and discovery of the gastrointestinal metastasis. There are two small clinical series that included patients who underwent resection of a gastrointestinal metastasis (Table 2). Three long-term survivors after resection were described in those reports. In contrast to the survivors in the current study, one of those patients had synchronous gastrointestinal metastases and two had multiple metastatic lesions outside the gastrointestinal tract. These conflicting data indicated that a disease-free interval or the number of metastatic foci was not always a predictor for long survival after resection. More clinical information is therefore necessary to identify indicators to select optimal patients for resection of gastrointestinal metastasis.

Conclusion

Although an initial recurrence of NSCLC after complete resection rarely develops in gastrointestinal organs, it

Table 2 Summary of previous and present reports in gastrointestinal metastases

Study	No. of cases	Surgery for GI metastasis (yes/no)	Interval between diagnosis of lung cancer and discovery of GI metastasis (mean)	Median Survival (median)	Survival duration after surgery	Long-survivors after GI surgery
Berger (1997)	7	6/1	11.2 months	120.0 days	7.5 months	Alive at 22 months ($M = 1$)
Kim (2009)	10	6/4	147.0 days	96.5 days	17.5 months	Alive at 33 and 63 months ($M = 2$)
Present report	9	5/4	6.9 months	10.8 months	27.7 months	Shown in Table 1

may nevertheless cause life-threatening symptoms and lead to shortened survival. Surgical resection of gastrointestinal metastasis is indicated not only for symptom relief but for providing the potential of a long-term survival if the patients are properly selected.

References

1. Arriagada R, Bergman B, Dunant A, Le Chevalier T, Pignon JP, Vansteenkiste J. Cisplatin-based adjuvant chemotherapy in patients with completely resected non-small-cell lung cancer. N Engl J Med 2004;350:351–60.
2. Ichinose Y, Yano T, Yokoyama H, Inoue T, Asoh H, Tayama K, et al. Postrecurrent survival of patients with non-small-cell lung cancer undergoing a complete resection. J Thorac Cardiovasc Surg 1994;108:158–61.
3. Garwood RA, Sawyer MD, Ledesma EJ, Foley E, Claridge JA. A case and review of bowel perforation secondary to metastatic lung cancer. Am Surg 2005;71:110–6.
4. Yang CJ, Hwang JJ, Kang WY, Chong IW, Wang TH, Sheu CC, et al. Gastro-intestinal metastasis of primary lung carcinoma: clinical presentations and outcome. Lung Cancer 2006; 54:319–23.
5. Porte H, Siat J, Guibert B, Lepimpec-Barthes F, Jancovici R, Bernard A, et al. Resection of adrenal metastases from non-small cell lung cancer: a multicenter study. Ann Thorac Surg 2001;71:981–5.
6. Granone P, Margaritora S, D'Andrilli A, Cesario A, Kawamukai K, Meacci E. Non-small cell lung cancer with single brain metastasis: the role of surgical treatment. Eur J Cardiothorac Surg 2001;20:361–6.
7. Sugimura H, Nichols FC, Yang P, Allen MS, Cassivi SD, Deschamps C, et al. Survival after recurrent nonsmall-cell lung cancer after complete pulmonary resection. Ann Thorac Surg 2007;83:409–17; discussioin 417–18.
8. Kim MS, Kook EH, Ahn SH, Jeon SY, Yoon JH, Han MS, et al. Gastrointestinal metastasis of lung cancer with special emphasis on a long-term survivor after operation. J Cancer Res Clin Oncol 2009;135:297–301.
9. Berger A, Cellier C, Daniel C, Kron C, Riquet M, Barbier JP, et al. Small bowel metastases from primary carcinoma of the lung: clinical findings and outcome. Am J Gastroenterol 1999;94:1884–7.
10. McNeill PM, Wagman LD, Neifeld JP. Small bowel metastases from primary carcinoma of the lung. Cancer 1987;59: 1486–9.
11. Yoshino I, Yohena T, Kitajima M, Ushijima C, Nishioka K, Ichinose Y, et al. Survival of non-small cell lung cancer patients with postoperative recurrence at distant organs. Ann Thorac Cardiovasc Surg 2001;7:204–9.
12. Yoshimoto A, Kasahara K, Kawashima A. Gastrointestinal metastases from primary lung cancer. Eur J Cancer 2006;42: 3157–60.
13. Antler AS, Ough Y, Pitchumoni CS, Davidian M, Thelmo W. Gastrointestinal metastases from malignant tumors of the lung. Cancer 1982;49:170–2.
14. Yuen JS, Chow PK, Ahmed Q. Metastatic lung cancer causing bowel perforations: spontaneous or chemotherapy-related? ANZ J Surg 2002;72:245–6.

Hepatocyte Growth Factor Expression in *EGFR* Mutant Lung Cancer with Intrinsic and Acquired Resistance to Tyrosine Kinase Inhibitors in a Japanese Cohort

Seiji Yano, MD, PhD, Tadaaki Yamada, MD, PhD,* Shinji Takeuchi, MD, PhD,* Keisei Tachibana, MD, PhD,† Yuko Minami, MD, PhD,† Yasushi Yatabe, MD, PhD,‡ Tetsuya Mitsudomi, MD, PhD,§ Hidenori Tanaka, MD, PhD,‖ Tatsuo Kimura, MD, PhD,‖ Shinzoh Kudoh, MD, PhD,‖ Hiroshi Nokihara, MD, PhD,¶ Yuichiro Ohe, MD, PhD,¶ Jun Yokota, MD, PhD,# Hidetaka Uramoto, MD, PhD,** Kosei Yasumoto, MD, PhD,** Katsuyuki Kiura, MD, PhD,†† Masahiko Higashiyama, MD, PhD,‡‡ Makoto Oda, MD, PhD,§§ Haruhiro Saito, MD, PhD,‖‖ Junji Yoshida, MD, PhD,¶¶ Kazuya Kondoh, MD, PhD,## and Masayuki Noguchi, MD, PhD†*

Introduction: This study was performed to determine the incidence rates of resistance factors, i.e., high-level hepatocyte growth factor (HGF) expression, epidermal growth factor receptor (EGFR) T790M secondary mutation, and *MET* amplification, in tumors with intrinsic and acquired EGFR tyrosine kinase inhibitor (TKI) resistance in *EGFR* mutant lung cancer.

Methods: Ninety-seven specimens from 93 *EGFR* mutant lung cancer patients (23 tumors with acquired resistance from 20 patients, 45 tumors with intrinsic resistance from 44 patients [nonresponders], 29 sensitive tumors from 29 patients) from 11 institutes in Japan were analyzed. HGF expression, *EGFR* T790M secondary mutation, and *MET* amplification were determined by immunohistochemistry, cycleave real-time polymerase chain reaction, and fluorescence in situ hybridization, respectively.

Results: High-level HGF expression, *EGFR* T790M secondary mutation, and *MET* amplification were detected in 61, 52, and 9% of tumors with acquired resistance, respectively. High-level HGF expression was detected in 29% of tumors with intrinsic resistance (nonresponders), whereas *EGFR* T790M secondary mutation and *MET* amplification were detected in 0 and 4%, respectively. HGF expression was significantly higher in tumors with acquired resistance than in sensitive tumors ($p < 0.001$, Student's t test). Fifty percent of tumors with acquired resistance showed simultaneous HGF expression with *EGFR* T790M secondary mutation and *MET* amplification.

Conclusions: High-level HGF expression was detected more frequently than *EGFR* T790M secondary mutation or *MET* amplification in tumors with intrinsic and acquired EGFR-TKI resistance in *EGFR* mutant lung cancer in Japanese patients. These observations provide a rationale for targeting HGF in EGFR-TKI resistance in *EGFR* mutant lung cancer.

Key Words: EGFR-TKI, EGFR mutation, HGF, Acquired resistance, Intrinsic resistance.

(*J Thorac Oncol.* 2011;X: 000–000)

*Division of Medical Oncology, Cancer Research Institute, Kanazawa University, Takara-machi, Kanazawa; †Department of Pathology, Institute of Basic Medical Sciences, University of Tsukuba, Tsukuba, Ibaraki; ‡Department of Pathology and Molecular Diagnosis; §Department of Thoracic Surgery, Aichi Cancer Center Hospital, Nagoya, Aichi; ‖Department of Respiratory Medicine, Graduate School of Medicine, Osaka City University, Sumiyoshi-ku, Osaka; ¶Division of Internal Medicine and Thoracic Oncology; #Division of Biology, National Cancer Center Hospital, Tokyo; **Second Department of Surgery, University of Occupational and Environmental Health, Kitakyushu; ††Department of Hematology, Oncology, and Respiratory Medicine, Okayama University Graduate School of Medicine, Okayama; ‡‡Department of Thoracic Surgery, Osaka Medical Center for Cancer and Cardiovascular Diseases, Osaka, Osaka; §§Department of Thoracic Surgery, Kanazawa University Hospital, Takara-machi, Kanazawa; ‖‖Department of Thoracic Oncology, Kanagawa Cancer Center, Yokohama; ¶¶Department of Thoracic Oncology, National Cancer Center Hospital East, Kashiwa, Chiba; and ##Department of Thoracic, Endocrine Surgery and Oncology, Institute of Health Bioscience, The University of Tokushima Graduate School, Tokushima, Japan.

Disclosure: Seiji Yano has received honoraria and research funding from Chugai Pharma.

Address for correspondence: Seiji Yano, Division of Medical Oncology, Cancer Research Institute, Kanazawa University, 13-1 Takara-machi, Kanazawa, Ishikawa 920-0934, Japan. E-mail: syano@staff.kanazawa-u.ac.jp

ISSN: 1556-0864/11/0000-0001

Epidermal growth factor receptor (EGFR)-activating mutations, in-frame deletion in exon 19, and L858 point mutation in exon 21 are selectively expressed in a population with lung cancer.[1,2] *EGFR*-activating mutations are detected considerably more frequently in nonsmokers, females, adenocarcinomas, and patients from East Asia, including Japan.[3–5] The reversible EGFR tyrosine kinase inhibitors (EGFR-TKIs) gefitinib and erlotinib show dramatic therapeutic efficacy, response rates of 70 to 80%, and significant prolongation of progression-free survival (PFS) compared

with standard first-line cytotoxic chemotherapy in patients with *EGFR* mutant lung cancer.[6–9] However, patients almost always develop acquired resistance to EGFR-TKIs after varying periods.[6,9,10] In addition, 20 to 30% of patients with *EGFR*-activating mutations show intrinsic resistance to EGFR-TKIs.[4] Therefore, intrinsic and acquired resistance to EGFR-TKIs are major problems in management of *EGFR* mutant lung cancer.

Two genetically conferred mechanisms—*EGFR* T790M secondary mutation (T790M secondary mutation)[11,12] and *MET* gene amplification[13]—induce acquired resistance to EGFR-TKIs in *EGFR* mutant lung cancer. In addition, we recently demonstrated the occurrence of hepatocyte growth factor (HGF)-induced resistance.[14] HGF, a ligand of MET,[15] induces EGFR-TKI resistance by activating MET, which restores phosphorylation of downstream MAPK-ERK1/2 and PI3K-Akt pathways,[14] using Gab1 as an adaptor.[16] HGF may be involved in both intrinsic and acquired resistance to EGFR-TKIs in *EGFR* mutant lung cancer.[14]

T790M secondary mutation, *MET* amplification, and high-level HGF expression were detected in clinical specimens from *EGFR* mutant lung cancer patients who acquired resistance to EGFR-TKIs,[11–14,16–18] indicating the clinical relevance of all three resistance mechanisms in lung cancer. Although the number of cases in each study was limited (<30 cases/study), probably because of low availability of biopsy specimens from resistant tumors, *EGFR* T790M secondary mutation and *MET* amplification were estimated to have occurrence rates of 50%[11,12,17,19] and up to 20%,[13,16,17] respectively, in patients showing acquired resistance to EGFR-TKIs. Nevertheless, the incidence of HGF-induced resistance has not been determined. In addition, the incidence rates of these three resistance factors in intrinsic resistance (nonresponders) are unknown.

Here, we performed a large-scale study in 23 tumors with acquired resistance from 20 patients, 45 tumors with intrinsic resistance from 44 patients (nonresponders), and 29 sensitive tumors from 29 patients to determine the incidences of the three resistance factors not only in acquired resistance but also in intrinsic resistance (nonresponders) to EGFR-TKIs in Japanese patients with *EGFR* mutant lung cancer.

MATERIALS AND METHODS

Patient details are described in the Supplementary information (http://links.lww.com/JTO/A197).

Definition of Sensitivity to EGFR TKI

Here, tumors with *EGFR* mutation known to be associated with drug sensitivity (i.e., G719X, exon 19 deletion, and L858R) were obtained from patients before or after treatment with a single EGFR-TKI.[9]

Sensitive tumors were defined as those obtained from patients whose tumors showed a decrease in diameter of at least 30% (either documented partial response or complete response) associated with EGFR-TKI treatment in imaging studies (Response Evaluation Criteria in Solid Tumors [RECIST] version 1.0). Tumor specimens were obtained before EGFR-TKI treatment.

Tumors with acquired resistance were defined as described previously.[9] Briefly, cases showing objective clinical benefit from treatment with an EGFR TKI as defined by either documented partial or complete response (RECIST) or significant and durable (>6 months) clinical benefit (stable disease as defined by RECIST) and systemic progression of disease (RECIST), while on continuous treatment with gefitinib or erlotinib within the last 30 days were defined as showing acquired resistance. Tumor specimens were obtained after systemic progression of disease.

As intrinsic resistance (nonresponders) has not been clearly defined, tumors without response to treatment with an EGFR TKI, i.e., either documented stable disease or progressive disease (RECIST), were defined as showing intrinsic resistance (nonresponders). Tumor specimens were obtained either before or after EGFR-TKI treatment.

Patients

Ninety-seven tumor specimens with EGFR mutations were obtained from 93 lung cancer patients, all of whom provided written informed consent, at 11 institutes in Japan. This study was approved by the Institutional Review Boards of each institute.

Patients' characteristics are shown in Table 1. Eighty-seven patients had adenocarcinomas, one had large cell carcinoma, two had squamous cell carcinoma, two had adenosquamous carcinoma, and one had undifferentiated non-small cell carcinoma. As the first EGFR-TKI, gefitinib and erlotinib were given to 82 and 10 patients, respectively, and the dual inhibitor of EGFR and VEGFR2, vandetanib,[20] was given to 1 patient.

Exon 19 deletion and L858R point mutation in exon 21 of *EGFR* were detected in 40 and 57 of the 97 tumors, respectively (Table 1). Two of these tumors had both exon 19 deletion and L858R point mutation. Two tumors without exon 19 deletion or L858R had G719X. Twenty-three tumors with acquired resistance were obtained from 20 patients after EGFR-TKI treatment. Forty-five tumors with intrinsic resistance (nonresponders) were obtained from 44 patients either before (41 tumors from 41 patients) or after (four tumors from three patients) EGFR-TKI treatment. Twenty-nine sensitive tumors were obtained from 29 patients before EGFR-TKI treatment.

Immunohistochemistry for HGF

Immunohistochemical staining was conducted on formalin-fixed, paraffin-embedded tissue sections (4 μm thick) of tumor specimens with microwave antigen retrieval in 0.01 M citrate buffer (pH 6.0). We used rabbit polyclonal antibody against HGF-α (IBL, Gunma, Japan) at 1:20 dilution as a primary antibody and EnVision/HRP Polymer Reagent (Dako, Glostrup, Denmark) and DAB (3,3′-diaminobenzidine tetrahydrochloride) Liquid (Dako) for detection.

Evaluation of HGF Expression

The percentages of cancer cells with positive cytoplasmic and/or membrane HGF immunoreactivity were evaluated (0 to 100%), and the modal intensity of the positively staining cells on a scale ranged from 0 to 3+ (0, complete